ACS Infectious Diseases

pubs.acs.org/journal/aidcbc

Article

ClpC1 Modulating Ohmyungsamycin A and Ecumicin Natural Product Analogues are Potent Antimycobacterials

Published as part of ACS Infectious Diseases special issue "Combating Tuberculosis: Obstacles, Innovations, and the Road Ahead".

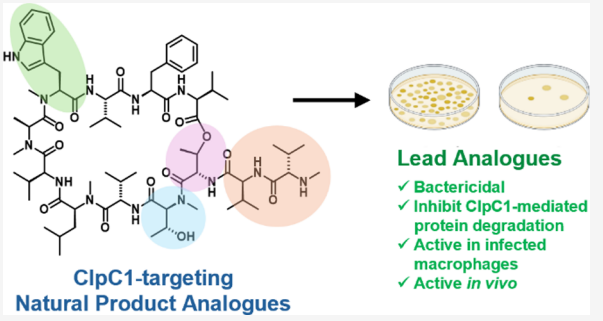
Paige M. E. Hawkins, Max J. Bedding, David M. Hoi, Isabel K. Barter, Chen-Yi Cheung, Stefan H. Oehlers, Gregory M. Cook, Tim Clausen, Warwick J. Britton, and Richard J. Payne*

Cite This: https://doi.org/10.1021/acsinfecdis.5c00689

Read Online

ACCESS | Metrics & More | Article Recommendations | Supporting Information

ABSTRACT: Herein, we describe the design, synthesis, and evaluation of modified cyclic peptides based upon the privileged structure of the cyclic depsipeptide natural products, ohmyungsamycin and ecumicin, that target *Mycobacterium tuberculosis* (*Mtb*) caseinolytic-like protein 1 (ClpC1). Simplified analogues featuring substitution at three sites (L-Thr-3, *N*-Me-L-Trp-9, and/or the N-terminus) were designed and synthesized via a novel and robust strategy, employing an oxazolidine-protected C-terminal amino acid, to enable late-stage, epimerization-free, solution-phase macrolactamization. Lead analogues had nanomolar affinity for the ClpC1 N-terminal domain (NTD), possessed potent activity against *Mtb* in vitro and were shown to inhibit protein degradation by the mycobacterial ClpC1:ClpP1P2 protease with an associated enhancement of ClpC1 ATPase activity. The most promising analogue from the series exhibited prolonged bactericidal killing activity against *Mtb* without the emergence of resistance and retained activity in an in vivo zebrafish model of mycobacterial infection.



KEYWORDS: *Mycobacterium tuberculosis, proteolysis, ClpC1, cyclic peptides, natural products*

Mycobacterium tuberculosis (*Mtb*) is the causative agent of tuberculosis (TB), and is the leading cause of death by an infectious disease worldwide, resulting in 1.25 million deaths and over 10 million new infections in 2023.[1] TB has been globally acknowledged as a disease that urgently needs attention with world leaders at the UN's first-ever high-level meeting on TB[2] affirming their commitment to the United Nations Sustainable Development Goals (to end the TB pandemic by 2030)[3] and the 'End TB Strategy' from the World Health Organization (WHO).[4] The existence of international collaborations on this scale underscore the urgency of the health problem; in line with achieving these goals the UN Secretary-General's 2020 progress report recommends urgent prioritization of ten actions to meet global targets, including increased investment in research and development and addressing the drug-resistant TB crisis.[5]

Treatment of multidrug-resistant (MDR) and extensively drug-resistant (XDR) TB is complex. Currently it is recommended to administer a fluoroquinolone antibiotic, bedaquiline and at least two other antibiotics over a period of 9−20 months. The new 6 month regimen has received conditional recommendation by WHO and includes the use of the most recently approved TB drug, pretomanid or delamanid.[6] Unfortunately, TB treatment compliance is often poor due to the long and complex drug regimens and the toxicity of several second-line TB drugs. This poor compliance has led to the ongoing development of resistance to current and novel drugs. As a result of these challenges, there is an urgent need for new antimycobacterial agents that operate via novel modes of action and that show rapid bactericidal activity in order to shorten the duration of TB treatment regimens.[7,8]

A family of structurally related cyclic depsipeptide natural products ohmyungsamycin A (**1**),[9−12] ecumicin (**2**),[11,13−15] and deoxyecumicin (**3**)[11,16] have shown promise as antimycobacterials both in vitro and in vivo (Figure 1A). Importantly, ecumicin has been shown to bind to and dysregulate the activity of the N-terminal domain (NTD) of an *Mtb* chaperone protein ClpC1 that is not currently the target of any TB drugs.[14,17] ClpC1 is an ATPase that binds to

Received: August 8, 2025
Revised: October 7, 2025
Accepted: October 9, 2025

ACS Publications © XXXX American Chemical Society

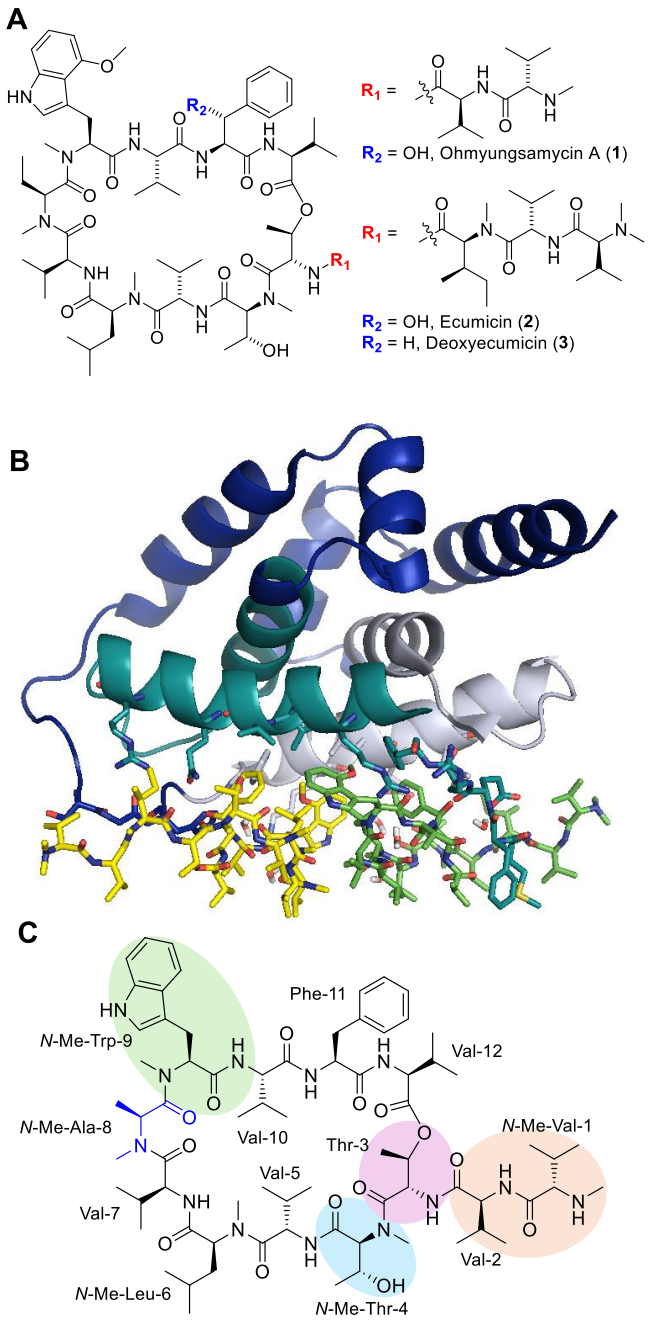


Figure 1. (A) Structure of the natural products ohmyungsamycin A (**1**), ecumicin (**2**), and deoxyecumicin (**3**); (B) cocrystal structure of two ecumicin (**2**) molecules (shown in yellow and green) bound to the NTD of ClpC1 (blue, showing NTD repeat 1 (cyan) and NTD repeat 2 (gray) (PDB: 6PBS[17]); and (C) structure of lead desmethoxydeoxy analogue **Ecu* 4** featuring an *N*-Me-L-Val-8 to *N*-Me-L-Ala-8 substitution (blue).[25] Colored circles show proposed substitution sites for next-generation analogues. *N*-methylation of *N*-Me-L-Thr-4 (blue); substitution at L-Thr-3 (purple); substitution at *N*-Me-L-Trp-9 (green); and substitution at the N-terminus (orange).

and regulates the proteolytic activity of the ClpP1P2 protease complex.[14,17] This complex is implicated in the elimination of misfolded and unfolded proteins and is essential for cell viability in mycobacteria but not in other pathogenic bacteria, making the proteins within the Clp complex attractive drug targets for the development of highly selective antimycobacterials.[18−22] Interestingly, based on a recently solved structure, ecumicin appears to bind to ClpC1 in a 1:2 target:ligand stoichiometry and this binding triggers significant conformational changes in the NTD of the protein (Figure 1B).[17,23,24] This binding is hypothesized to alter the ClpC1-mediated ClpP1P2 proteolytic activity, increasing ATP hydrolysis and dysregulating proteolysis. It is the subsequent dysregulation of protein homeostasis that is proposed to lead to cell death.[14]

Recently, we reported simplified desmethoxydeoxy analogues of the cyclic depsipeptide natural products ohmyungsamycin A (**1**)[9,10] and ecumicin (**2**)[13,16] whereby the 4-OMe-*N*-Me-L-Trp at residue 9 and the *β*−OH-L-Phe at residue 11 were replaced with *N*-Me-L-Trp and L-Phe, respectively (Figure 1C).[25] These proved to be potent antimycobacterials in vitro (MIC = 125−500 nM against *Mtb*) and maintained *Mtb* inhibitory activity in macrophages where mycobacteria reside in vivo. Finally, each of the analogues was shown to inhibit protein degradation of the ClpC1-mediated ClpP1P2 protease system, consistent with the mechanism of action of the parent natural products. The most promising analogue from this series (**Ecu* 4**), possessing an *N*-Me-L-Val-8 to *N*-Me-L-Ala substitution (Figure 1C), exhibited rapid bactericidal killing activity against *Mtb* strain mc^{2}6230 (Δ*RD1* Δ*panCD*), capable of sterilizing cultures after 7 days. This analogue also retained activity against hypoxic *Mtb* and could inhibit mycobacterial infection in a zebrafish model.[25,26] Based on these promising results, we sought to design and synthesize a second-generation series of analogues using lead analogue **Ecu* 4** (previously referred to as "analogue **6**") as a starting point.[25]

Early attempts at synthesizing analogues that possessed substitutions at other residues via our previously established route (loading of the C-terminal Fmoc-L-Phe-OH onto hyper acid-labile resin and subsequent Fmoc-SPPS, resin cleavage and macrolactamization)[25] failed to deliver the target molecules in satisfactory yield and purity. This was due in major part to susceptibility of the analogues to macrolactone hydrolysis and/or C-terminal epimerization during the cyclization step. To address this, we sought to develop an improved synthetic route to prevent C-terminal epimerization, while simultaneously delivering more stable second-generation analogues by substituting the depsipeptide ester linkage for an amide bioisostere. Importantly, not only would the ester to amide substitution enhance the stability of analogues to chemical and enzymatic hydrolysis, it would also circumvent the need for a challenging on-resin esterification step, simplifying synthesis and minimizing the chance of epimerization of the target molecules.

Natural product analogue design was guided by both the published structure of the ClpC1-ecumicin complex[17] and published antimycobacterial data of prior analogues[12] and led to the design of two distinct analogue series whereby the *N*-Me-L-Trp residue at residue 9 and the N-terminus of **Ecu* 4** (residues 1 and 2) were substituted. The resulting series of analogues were synthesized via our modified synthetic route and evaluated against ClpC1 and *Mtb* in order to probe structure−activity relationships (SARs). Several promising candidates emerged from this study with impressive antimycobacterial activity in vitro and in vivo.

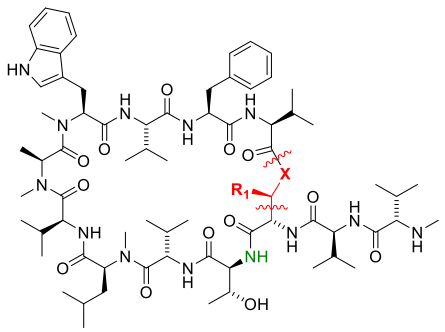
RESULTS AND DISCUSSION

Preventing C-Terminal Epimerization. In order to overcome the aforementioned C-terminal epimerization during synthesis we proposed a new synthetic route to the natural product analogues via oxazolidine protection of the C-terminal

https://doi.org/10.1021/acsinfecdis.5c00689
ACS Infect. Dis. XXXX, XXX, XXX−XXX

amino acid residue.[27−30] Oxazolidines prevent racemization of C-terminal amino acids in two ways: (1) via the major oxazolone pathway that can no longer occur due to the presence of a tertiary substituted amine that cannot be deprotonated to generate the imine; and (2) inhibition of racemization via an enolization pathway due to the unfavorable formation of a highly strained enol. Oxazolidines are also traceless amino acid protecting groups that can be removed during the final acidic deprotection of a peptide and, as such, would not have any detrimental impact on the overall secondary structure of the cyclic peptide.[27−30] Importantly, lead analogue **Ecu* 4** contains one good candidate for oxazolidine protection, *N*-Me-L-Thr-4 (highlighted in blue, Figure 1C), however, the *N*-methyl functionality is not compatible with oxazolidine formation. As such, an analogue (**5**) lacking *N*-methylation at this position was first synthesized and pleasingly, was shown to retain tight binding to the ClpC1-NTD by surface plasmon resonance (SPR, K_D = 0.29 μM) and exhibit equipotent activity to **Ecu* 4** against *Mtb* in vitro (MIC = 0.5 μM, Table 1).

Table 1. Activity of Second-Generation Natural Product Analogues with Substitution at Residues 3 and 4 against ClpC1-NTD (Affinities Measured by SPR) and against *Mtb* Strain mc^{2}6230



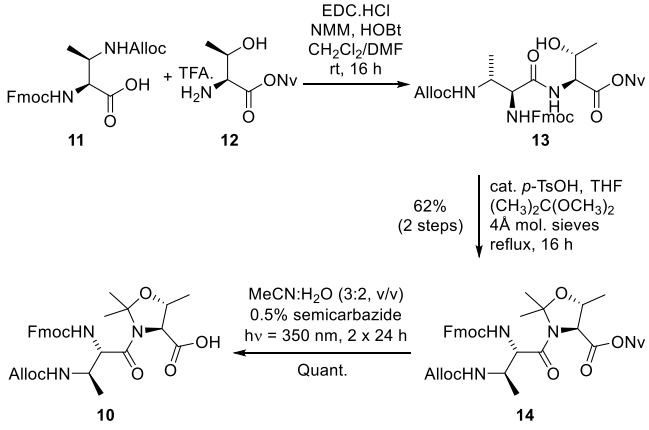
	Substitution	K_D (μM)	MIC (μM)		Substitution	K_D (μM)	MIC (μM)
5		0.29	0.5	**6**		0.38	1
7		0.61	4	**8**		0.32	0.5
9		0.89	1	**Ecu* 4**		0.39	0.5
				Isoniazid		N/A	0.2

Next, to prevent unwanted macrolactone hydrolysis during synthesis, we proposed substituting the native depsipeptide (ester) linkage for a bioisoteric amide through substitution of L-Thr-3 (highlighted in purple, Figure 1C); inspection of the cocrystal structure did not indicate any significant interactions between this residue and the NTD of ClpC1 and substitution was therefore thought to be tolerated.[17] To further elucidate the SAR at this position, several analogues were synthesized including those with substitution of L-Thr-3 with (2*S*,3*R*)-2,3 diaminobutanoic acid (DABA) (**6**), as well as L-2,3-diaminopropionic acid (L-DAP) (**7**) to generate an analogue lacking the β-methyl moiety. Two final analogues: N_β-methyl-DABA (**8**) and N_β-methyl-L-DAP (**9**) were also synthesized to remove the hydrogen bond donor capacity introduced in analogues **6** and **7** (which is not present in the depsipeptides) as this can influence cyclic peptide conformation and biological activity.[31]

It is worth noting that it is not possible to load the corresponding *iso*propylidene-protected Fmoc-L-Thr-OH-4 directly onto resin to initiate the Fmoc-SPPS, as subsequent Fmoc-deprotection and amino acid coupling to this residue results in the concomitant removal of the *iso*propylidene-protecting group, likely due to the *endo*-anomeric effect.[32] Fortunately, it is well-known that *N*-acyloxazolidines (such as pseudoproline dipeptides) reverse the *endo*-anomeric effect by conjugating the nitrogen lone pair with the carbonyl, increasing the stability of the *iso*propylidene.[32] As such, we synthesized suitably protected oxazolidine dipeptides, featuring an *iso*propylidene-protected L-Thr-4 and the adjacent L-DAP-3 or DABA-3 that could be used to synthesize the target macrolactam analogues **6**−**9**.

The desired oxazolidine-protected dipeptide **10** was synthesized following amidation of a suitably protected derivative of the noncanonical amino acid, DABA (**11**) (see Supporting Information for synthetic details), with 4,5-dimethoxy-2-nitrobenzyl (nitroveratryl/Nv)-protected L-Thr (**12**) (Scheme 1). The resulting dipeptide **13** was refluxed

Scheme 1. Synthesis of the Oxazolidine-Protected DABA-L-Thr Dipeptide 10



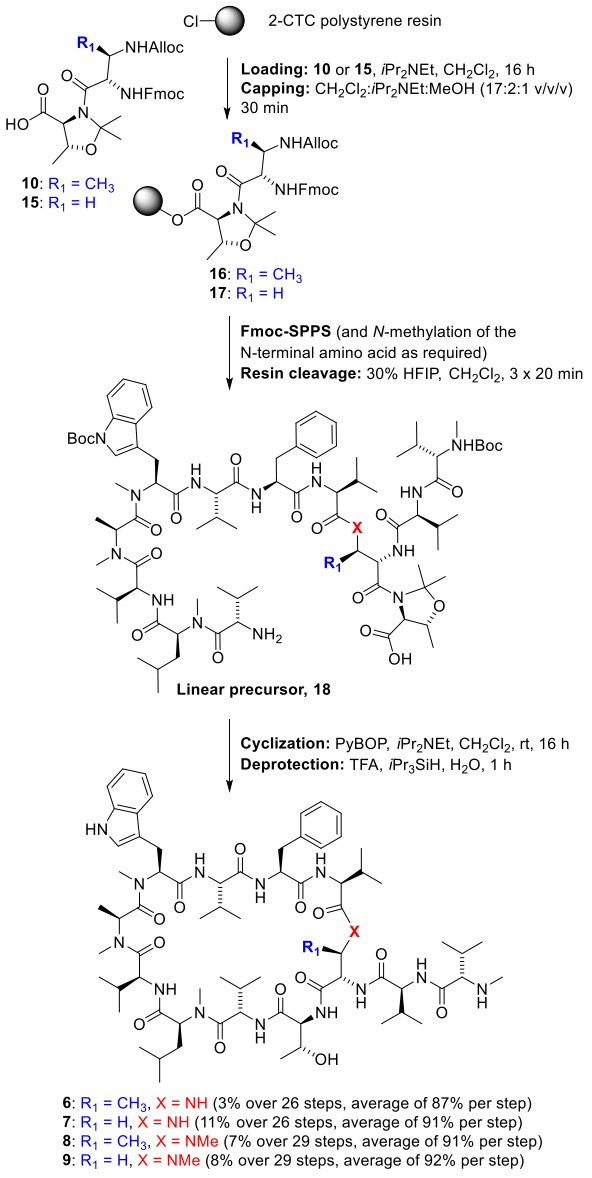
over 4 Å molecular sieves with 2,2-dimethoxypropane and an acid catalyst to provide the oxazolidine-protected dipeptide **14**. Removal of the Nv-group via irradiation at 350 nm in the presence of semicarbazide as an aldehyde scavenger provided the desired dipeptide **10**, ready for incorporation into a cyclic peptide analogue. It should be noted that the dipeptide was orthogonally protected with an Fmoc-group on the N-terminus and an Alloc-group on the β-amine side chain to enable chemoselective deprotection on-resin.

Synthesis of the corresponding oxazolidine-protected L-DAP-L-Thr dipeptide **15** proceeded similarly starting from the commercially available amino acid, Fmoc-L-DAP(Alloc)−OH (see Supporting Information for the synthesis of dipeptide **15**).

With the target dipeptides in hand, synthesis of the natural product analogues **6**−**9** could commence; this began with the loading of **10** and **15** onto 2-CTC resin to provide **16** and **17**, respectively (see Scheme 2 for general synthetic route). It should be noted that the use of the bulky 2-CTC resin was particularly important in minimizing diketopiperazine formation when deprotecting resin-bound dipeptides **16** and **17**. The resin-bound dipeptides were elongated by Fmoc-SPPS on the N-terminus, through iterative cycles of Fmoc-deprotection

https://doi.org/10.1021/acsinfecdis.5c00689
ACS Infect. Dis. XXXX, XXX, XXX−XXX

Scheme 2. Synthesis of Cyclic Peptide Analogues 6−9



with piperidine in DMF and amino acid coupling using 1-[*bis*(dimethylamino)methylene]-1*H*-1,2,3-triazolo[4,5b]-pyridinium 3-oxid hexafluorophosphate (HATU) as the coupling agent and *N*,*N*-di*iso*propylethylamine as the base. Alloc-deprotection of the β-amine using catalytic $Pd(PPh_3)_4$ with phenylsilane as a scavenger preceded a three-step on-resin *N*-methylation of the β-amine of DABA-3/L-DAP-3 and/or L-Trp-9 using (1) nosyl (Ns) chloride and *sym*-collidine to activate the requisite amine, (2) Mitsunobu reagents (PPh_3, di*iso*propyl azodicarboxylate (DIAD) and MeOH) to perform the methylation, and (3) 2-mercaptoethanol with 1,8-diazabicyclo[5.4.0]undec-7-ene (DBU) to remove the Ns-group.[33]

Following this, the peptides were cleaved from resin with 1,1,1,3,3,3-hexafluoroisopropanol (HFIP) to provide the linear peptide precursors for each analogue (general structure **18**). This linear precursor was subjected to macrolactamization using benzotriazole-1-yl-oxy-tris-pyrrolidino-phosphonium hexafluorophosphate (PyBOP) and iPr_2NEt in CH_2Cl_2, followed by deprotection with trifluoroacetic acid (TFA) to afford the desired analogues **6-9** after RP-HPLC purification (3−11% over 26−29 steps, average of 87−92% per step).

Having synthesized the target macrolactam natural product analogues **6−9**, we next evaluated their activity against *Mtb* strain mc^{2}6230 (Δ*RD1* Δ*panCD*) in vitro (Table 1). Strain mc^{2}6230 (Δ*RD1* Δ*panCD*) is an avirulent auxotrophic *Mtb* mutant that behaves identically to wild-type *Mtb* strain H37Rv when grown in pantothenate-supplemented medium, but is incapable of causing disease even in severe combined immunodeficiency (SCID) mice.[34] Pleasingly, analogues showed comparable activity to ecumicin (**2**) and first-generation analogue **Ecu* 4** which were used as positive controls. This series of analogues enabled the importance of the β-methyl group at residue 3 to be established, with a 4 to 8-fold loss in activity between analogues **6** and **7**. Additionally, a slight loss in activity could be observed when switching from L-Thr-3 to DABA-3 (**5** vs **6**); however, this activity was retained when the hydrogen bond donating capacity of DABA was removed in analogue **8** possessing *N*-methylation. Similar results were observed with the L-DAP-substituted analogue **7**, with *N*-methylation of the amide (**9**) regaining some of the activity lost by removal of the β-methyl group. Interestingly, the measured binding affinities of **6−9** to ClpC1-NTD by SPR were not substantially different to that of **Ecu* 4** (highlighted in Table 1). Given that the cocrystal structure did not indicate any significant interactions between this residue and the NTD of ClpC1[17] it is possible that the observed SAR is due to the methyl group imparting more favorable cell permeability over the nonmethylated counterparts. Finally, we found that substitution of the depsipeptide linkage to the more stable amide bioisostere, i.e., L-DAP in **7** and DABA in **6** was not deleterious to activity and was therefore deemed a suitable substitution for natural product analogues that would not be susceptible to macrolactone hydrolysis during synthesis. We chose to move forward with L-DAP substitution at residue 3 for future analogue generation, due to the commercial availability of this amino acid, which would enable the rapid synthesis of a larger number of analogues.

Substitution at *N*-Me-L-Trp-9. Analysis of the cocrystal structure of the ClpC1-ecumicin complex revealed a key cation-π interaction between the indole ring of *N*-Me-4-OMe-L-Trp of ecumicin and Arg-10 of ClpC1, as well as an additional cation-π interaction between the indole ring of *N*-Me-4-OMe-L-Trp from the second ecumicin molecule and ClpC1 Lys-85 (Figure 2).[17] To probe these interactions, we designed a six-member analogue series where the *N*-Me-L-Trp-9 residue (highlighted in green, Figure 1C) was substituted with various aromatic side chains (**19−21**) − including analogues with increased flexibility or decreased rotational freedom (**20−21**), polar or charged side chains (**22−23**), and an *N*-Me-L-Ala substitution (**24**) to ascertain the importance of this cation−π interaction for the antimycobacterial activity of the analogues. The target natural product analogues were next synthesized via the optimized protocol developed above and isolated in 2−7% yield over the 23−26 steps (average of 84−90% per step).

Synthetic analogues **19−24** were then evaluated for binding affinity to ClpC1-NTD by SPR (Table 2). A significant loss in binding affinity was observed for almost all substitutions (K_D > 10 μM for **20−24**), with only the *N*′-methylated **19** retaining ClpC1 binding, albeit with substantially diminished affinity (K_D = 2.4 μM). Screening these compounds (**19−24**) against *Mtb* strain mc^{2}6230 (Δ*RD1* Δ*panCD*) further supported the

https://doi.org/10.1021/acsinfecdis.5c00689
ACS Infect. Dis. XXXX, XXX, XXX−XXX

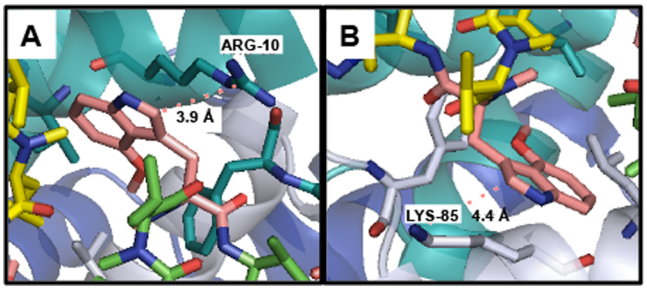
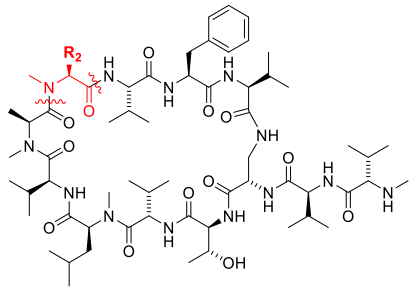
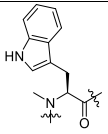
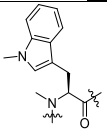
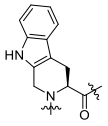
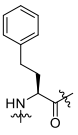
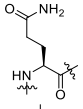
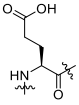


Figure 2. Zoomed in view of the cocrystal structure of two ecumicin molecules (shown in yellow and green, with *N*-Me-4-OMe-L-Trp shown in peach) bound to the NTD of ClpC1 (blue, with NTD repeat 1 (cyan) and NTD repeat 2 (gray) (PDB: 6PBS[17]) showing: (A) cation−π interaction between the indole ring of *N*-Me-4-OMe-L-Trp and ClpC1 Arg-10 and (B) putative cation-π stabilization between the indole ring of *N*-Me-4-OMe-L-Trp and ClpC1 Lys-85.

Table 2. Activity of *N*-Me-L-Trp-9 Substituted Natural Product Analogues against ClpC1-NTD (Affinities Measured by SPR) and against *Mtb* Strain mc^{2}6230



Substitution	K_D (μM)	MIC (μM)	Substitution	K_D (μM)	MIC (μM)
7 	0.61	4	**19** 	2.4	16
20 	>10	64	**21** 	>10	32
22 	>10	64	**23** 	>10	64
24 	>10	64	**Ecu* (4)**	0.39	0.5
			Isoniazid		0.2

293 importance of the *N*-Me-L-Trp residue for ClpC1-mediated
294 antimycobacterial activity. This was particularly evident with
295 analogue **24**, that possessed an Ala residue in place of Trp (in
296 parent analogue **7**) that resulted in a drastic loss in activity
297 (MIC = 64 μM). More modest changes, such as analogues
298 **19**−**21**, which should still be capable of facilitating the cation-π
299 interaction also resulted in significant activity loss (summarized
300 in Table 2). This suggests that an unsubstituted and
301 nonconformationally restricted indole side chain is important
302 for optimal interactions with ClpC1 (most likely the key
303 cation−π interaction with the ClpC1-NTD Arg-10 and/or Lys-
304 85 residues observed in the crystal structure). Lastly, analogues
305 **22** and **23** bearing polar/charged residues also exhibited a
306 dramatic loss in potency compared to parent analogue **7**.
307 Taken together, these data confirm the importance of the *N*-
308 methylTrp residue at position 9 for antimycobacterial activity.

309 **Substitution at the N-Terminus.** An acetylated analogue
310 of ohmyungsamycin A with a truncated N-terminus (R′ = Ac,
311 Figure 1A) was shown by Suh et al. to be 1000-fold less active
312 compared to the parent natural product.[12] Because the related
313 natural product ecumicin has a three amino acid residue N-
314 terminal 'head', compared to only two amino acid residues
315 present in ohmyungsamycin A (Figure 1A), we were interested
316 in exploring the role of N-terminal substitutions on activity
317 against ClpC1 and *Mtb*. Inspection of the ClpC1-ecumicin
318 structure revealed a key hydrogen bonding interaction between
319 a backbone carbonyl in Val-2 of one ecumicin molecule
320 (corresponding to *N*-Me-L-Val-1 in ohmyungsamycin A and
321 analogues) and the primary amine of Met1 in ClpC1 (Figure f3
322 3A).[17] Ecumicin also appears to form hydrophobic interactions

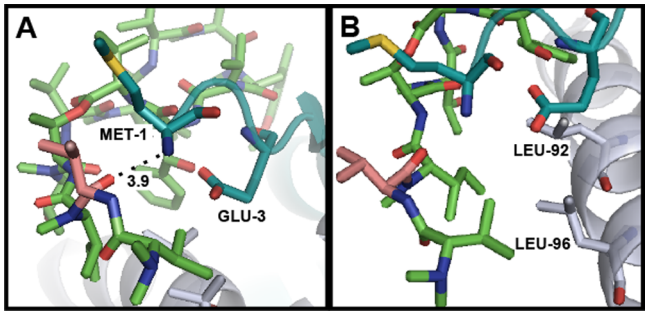


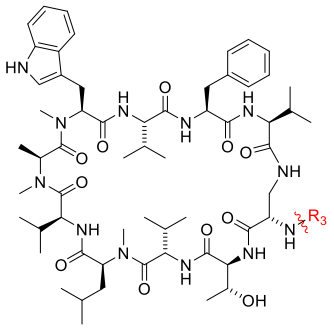
Figure 3. Zoomed in view of the cocrystal structure of one of two ecumicin molecules (shown in green, with L-Val-2 shown in peach) bound to the NTD of ClpC1 (blue, including NTD repeat 1 (cyan) and NTD repeat 2 (gray) (PDB: 6PBS[17]) showing: (A) hydrogen bond between the carbonyl of an ecumicin L-Val-2 and the N-terminus of ClpC1Met-1 and (B) ClpC1 Leu-92 and Leu-96 that may form hydrophobic interactions with the N-terminus of ecumicin.

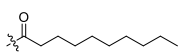
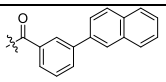
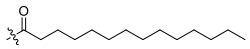
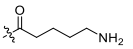
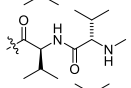
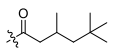
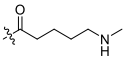
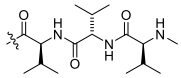
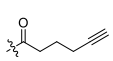
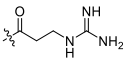
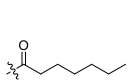
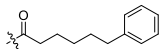
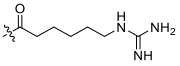
323 with the side chains of ClpC1 Leu-92 and Leu-96 (Figure 3B).
324 As such, we decided to investigate whether additional
325 interactions could be forged with neighboring residues to
326 improve antimycobacterial activity in a second series of natural
327 product analogues (highlighted in orange, Figure 1C).

328 Analogues were designed with a view to investigating the
329 effect of N-terminal length (**7**, **25**−**27**) and lipophilicity, with
330 flexible linear alkyl chains (**28**−**30**) and bulkier, conforma-
331 tionally restrained carbon chains (**31**−**34**) installed. Finally, a
332 small series with a range of basic residues (**35**−**38**) with
333 varying pKas were designed. The 15 natural product analogues
334 were first synthesized via the optimized solid-phase route
335 developed earlier (2−12% yield over 24−28 steps, average of
336 86−92% per step, see Supporting Information for details). To
337 expedite the synthesis, peptides featuring a fatty acid chain
338 were synthesized on-resin as the N-terminal Boc-protected
339 cyclic peptide core of **25**, cleaved, deprotected, and then
340 acylated in solution (see Supporting Information for full
341 synthetic details). With the 15 analogues in hand, they were
342 next evaluated for binding affinity to ClpC1-NTD and
343 antimycobacterial activity against *Mtb* strain mc^{2}6230 (Table t3
344 3). Modifications to the length of the N-terminus (**7**, **25**−**27**) t3
345 did not have a dramatic impact on potency. This was perhaps
346 surprising based on the large drop in potency observed in the

https://doi.org/10.1021/acsinfecdis.5c00689
ACS Infect. Dis. XXXX, XXX, XXX−XXX

Table 3. Activity of N-Terminal 'Head' Substituted Third-Generation Analogues against *Mtb* Strain mc^{2}6230



Substitution	K_D (μM)	MIC (μM)	Substitution	K_D (μM)	MIC (μM)	Substitution	K_D (μM)	MIC (μM)
25 	0.75	8	**29** 	>10	16	**34** 	>10	32
26 	0.72	8	**30** 	>10	64	**35** 	0.41	1
7 	0.61	4	**31** 	>10	32	**36** 	1.2	2
27 	9.5	2	**32** 	N.D.[a]	32	**37** 	0.77	0.5
28 	>10	64	**33** 	>10	32	**38** 	2.56	2
Ecu* **(4)**	0.39	0.5	Isoniazid		0.2			

[a] K_D could not be determined (N.D.) due to nonspecific binding.

'N-terminally truncated' analogue (R′ = Ac, Figure 1A) reported by Suh et al. (vide supra).[12] However, this may have been owing to the maintenance of the N-terminal amine in the analogues generated here. The addition of lipophilic carbon chains that capped the terminal amine functionality (**28**−**34**) also lost significant binding affinity and antimycobacterial activity irrespective of the flexibility, size, or aliphatic vs aromatic nature of the hydrocarbon chain (Table 3.). In contrast, alkyl chain analogues (**35**−**38**) terminating with basic functionalities (amines or guanidines) outperformed the analogues bearing standard amino acids in the N-terminus (**7**, **25**−**27**), with the most potent of these analogues, **37**, possessing a short-chain alkyl guanidine moiety (K_D = 0.77 μM, MIC = 0.5 μM). Taken together, these data suggest that a suitably positioned basic moiety is a critical functionality required for potent antimycobacterial activity of these natural product analogues. Upon inspection of the ecumicin-ClpC1 crystal structure there are no apparent interactions with the basic amine of ecumicin in the reported binding mode. However, it is plausible that an initial binding event of ecumicin (**2**, and related bioactive analogues **4**−**9**, **19**, **25**−**27**, and **35**−**38**) to ClpC1 would be driven by an ionic interaction between a protonated ammonium or guanidinium moiety on the peptide head and Glu3 in the disordered N-terminus of the protein (Figure 3A). This interaction could serve as an anchoring point to template formation of a favorable H-bonding network between the peptide and the N-terminal residues of ClpC1 (notably Met1, Phe2, Glu3, Phe5). Given the flexibility of this region of the protein and the observation that truncation (**25**−**26**) or alkyl chain substitution (**35**−**38**) was not detrimental to binding affinity, it is likely that the ligand−protein interaction involves dynamic conformational changes in both the peptide and protein, and that interactions made by a basic moiety (amine or guanidine) in the peptide head plays an important role in binding.

https://doi.org/10.1021/acsinfecdis.5c00689
ACS Infect. Dis. XXXX, XXX, XXX−XXX

Time-Kill Kinetics for Lead Analogues. Analogues **5**, **8**, and **37** that exhibited the most potent antimycobacterial activity from the various series were selected for further evaluation in a time-kill kinetic assays using *Mtb* strain mc^{2}6230 (Δ*RD1* Δ*panCD*) to assess bactericidal activity (Figure 4). The analogues compared favorably with the

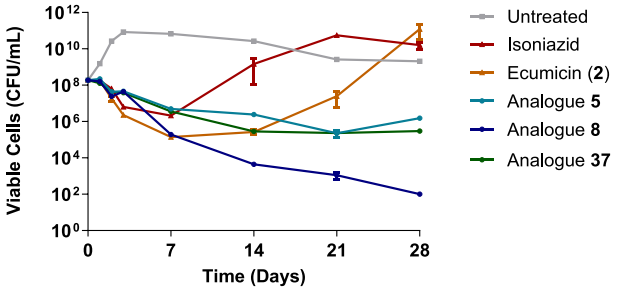


Figure 4. Time-kill kinetic assay of analogues **5**, **8**, and **37** against *Mtb* strain mc^{2}6230. Compound was administered to *Mtb* cells once at 10 × MIC, and cell viability was monitored for 28 days with 7H11 agar plate counts (CFU/mL). All experiments were performed in biological triplicates with the standard error of the mean shown.

positive control isoniazid,[35] with analogue **5** showing early bactericidal activity with resistance emerging after 14−21 days, analogous to ecumicin (**2**). Analogue **37** also showed early bactericidal activity for 14 or 21 days, however, unlike **5** analogue **37** remained bacteriostatic for the duration of the experiment. The most impressive analogue in the series was **8** that displayed bactericidal activity for the entire 28 days, with no emergence of bacterial tolerance.

Inhibition of ClpC1-Mediated Casein Degradation by the ClpP1P2 Protease Complex. We next assessed the ability of the lead analogues to inhibit the *Mycobacterium smegmatis* (*Msm*) ClpC1-mediated degradation of *β*-casein by the ClpP1P2 protease complex. Importantly, *Msm* ClpC1 and *Mtb* ClpC1 have high structural homology, with 100% sequence identity in the NTD. Previously, it has been reported that ecumicin (**2**) invokes a marked decrease in proteolysis of the phosphoprotein FITC casein of *Mtb* ClpC1.[14,25] Pleasingly, all lead natural product analogues (**5**, **8**, and **37**) also showed potent inhibition of *β*-casein degradation (see Supporting Information, Figure S1).

Measurement of ClpC1 ATPase Activity. We next proceeded to assess the effect of the analogues on the ATPase activity of *Msm* ClpC1 (Figure 5). Ecumicin (**2**) and our first-generation analogues increased the ATPase activity of ClpC1.[14,25] Similarly, lead analogues **5**, **8**, and **37** stimulated ATPase activity, with **5** and **8** stimulating a 2-fold change in ATPase activity at a concentration of 100 *μ*M, similar to previously reported lead analogue **Ecu* 4**.

In Vivo Studies. We next selected our most promising natural product analogues based on in vitro antimycobacterial activity (**8** and **37**) for assessment in an in vivo model of mycobacterial infection. Specifically, we employed a *M. marinum* zebrafish infection model which has been shown to be an effective alternative host system for evaluating *Mtb* infections.[36] Critically, *M. marinum* ClpC1 and *Mtb* ClpC1 also have a high structural homology, with identical NTD sequences. Zebrafish embryos were infected with tdTomato fluorescent *M. marinum* 2 days postfertilization and treated twice with **8** or **37** at 25 *μ*M on days four and five postinfection with analysis on the sixth day postinfection. Both **8** and **37**

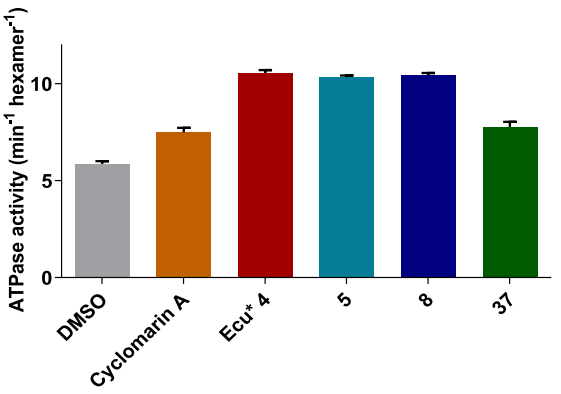


Figure 5. ATPase activity of *Msm* ClpC1. All analogues were assessed at a concentration of 100 *μ*M, with cyclomarin A as a positive control. All experiments were performed in biological triplicates with the standard error of the mean shown.

showed statistically significant inhibition of *M. marinum* in this in vivo model (Figure 6). Specifically, **8** and **37** exhibited a 41 and 37% reduction in the bacterial burden as compared to the DMSO control, respectively.

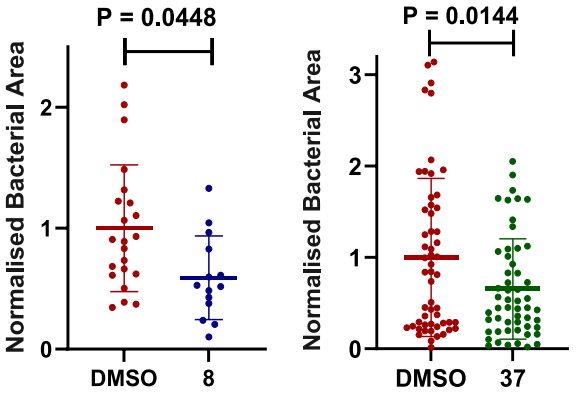


Figure 6. Activity of analogues **8** and **37** (25 *μ*M) in a *M. marinum* in vivo zebrafish model. Bacterial load was determined based on fluorescence in zebrafish embryos 6 days post infection (with treatment of **8**, **37**, or DMSO on days four and five). The standard deviation is shown and the difference between groups was analyzed by unpaired *t* and Mann−Whitney tests.

CONCLUSIONS

In summary, we have developed a robust epimerization-free synthetic strategy to access macrolactam analogues of the ohmyungsamycin A/ecumicin family of natural products. Three series of analogues were designed based on a prior lead analogue and the structure of the ecumicin-ClpC1 complex and probed the effect of substitution at L-Thr-3, *N*-Me-L-Trp-9 or the N-terminus. Through the synthesis and screening of these second-generation analogues, we found that the hydrolysis-prone depsipeptide linkage could be successfully substituted for an amide isostere while retaining ClpC1 binding affinity and antimycobacterial activity against *Mtb* in vitro. The importance of the *N*-Me-L-Trp residue was also revealed through a series of substitutions at this site. While the basic functionality at the N-terminus was found to be essential, the analogue with the most potent antimycobacterial activity (**37**, K_D = 0.77 *μ*M, MIC = 0.5 *μ*M) possessed a short alkyl chain that terminated in a guanidinium moiety in place of the

https://doi.org/10.1021/acsinfecdis.5c00689
ACS Infect. Dis. XXXX, XXX, XXX−XXX

peptide chain in the natural products. The most potent analogues from the series (**8** and **37**) were evaluated for their kinetics of mycobacterial killing, ClpC1-ClpP1P2-mediated protein degradation, and ClpC1 ATPase activity. Treatment of *Mtb* with **8** and **37** did not lead to the emergence of resistance after 28 days of treatment, with analogue **8** maintaining bactericidal activity for the duration of the experiment. Finally, analogues **8** and **37** were evaluated in an *in vivo* mycobacterial infection model in zebrafish. Both analogues were capable of reducing the *M. marinum* bacterial burden by 34−41% 2 days postadministration.

The SAR generated from this study, including the identification of two novel analogues **8** and **37**, which demonstrate superior antimycobacterial activity to the natural products, should prove useful in guiding the development of ClpC1-targeting TB drug candidates based on the privileged natural product scaffolds in the future.

MATERIALS AND METHODS

Chemistry. All reactions were carried out under an argon atmosphere and at room temperature (22 °C) unless the reaction was performed under aqueous conditions or unless otherwise specified. The reactions carried out at 0 °C employed a bath of water and ice. Anhydrous tetrahydrofuran (THF), CH_2Cl_2, MeOH, acetonitrile (MeCN), and dimethylformamide (DMF) were obtained using a PureSolv solvent purification system. The reactions were monitored by thin-layer chromatography (TLC) on aluminum backed silica plates (Merck Silica Gel 60 F254). Visualization of TLC plates was undertaken with an ultraviolet (UV) light at λ = 254 nm and staining with solutions of vanillin, ninhydrin, and potassium permanganate followed by exposure of the stained plates to heat. Silica flash column chromatography (Merck Silica Gel 60 40−63 μm) was undertaken to purify crude reaction mixtures using solvents as specified. Fractions were collected manually or with a Biotage Isolera Spektra automated flash purification system.

All commercially available reagents were used as obtained from Sigma-Aldrich, Merck, Acros Organics or AK Scientific. Amino acids, coupling reagents and 2-chlorotrityl chloride polystyrene resins were obtained from NovaBiochem, PCAS, GL Biochem, or Mimotopes and peptide synthesis grade DMF was obtained from Merck or Labscan. All noncommercially available reagents were synthesized according to literature procedures as referenced.

^{1}H NMR spectra were obtained using a Bruker AVIII 400, AVIII 500, or AVIII 800 with cryoprobe at frequencies of 400, 500, or 800 MHz respectively in $CDCl_3$, MeOD, acetone-d6, CD_3CN, or D_2O. Chemical shifts are reported in parts per million (ppm) and coupling constants in Hertz (Hz). ^{1}H NMR data is reported as follows: chemical shift values (ppm), multiplicity (s = singlet, d = doublet, t = triplet, q = quartet, m = multiplet, br = broad), coupling constant(s) and relative integral. ^{13}C NMR spectra were obtained using a Bruker AVIII 400, AVIII 500, or AVIII 800 with cryoprobe at 100, 125, or 200 MHz in $CDCl_3$, MeOD, or acetone-d6. ^{13}C NMR data is reported as chemical shift values (ppm). Any rotamers were confirmed via saturation transfer difference (STD) NMR experiments; however, due to the large number of cyclic peptide analogues synthesized only lead and select exemplar analogues were confirmed to be rotameric by STD-NMR experiments and additionally, only some of compounds were fully assigned by NMR using 1D- and 2D-NMR experiments.

Liquid chromatography−mass spectrometry (LC−MS) was performed on a Shimadzu 2020 UPLC-MS instrument with a Nexera X2 LC-30AD pump, a Nexera X2 SPDM30A UV−vis diode array detector, and a Shimadzu 2020 (ESI) mass spectrometer operating in either the positive or negative mode. Separations were performed on a Waters Acquity BEH300 1.7 μm, 2.1 mm × 50 mm (C18) column at a flow rate of 0.6 mL min^{-1}. Separations were performed using a mobile phase of 0.1 vol % FA in water (Solvent A) and 0.1 vol % FA in MeCN (Solvent B) using gradients as specified.

High-resolution mass spectra were recorded on a Bruker-Daltronics Apex Ultra 7.0T Fourier transform (FTICR) mass spectrometer.

Reversed-phase high-performance liquid chromatography (RP-HPLC) was performed on a Waters 600E multisolvent delivery system fitted with a Rheodyne 7725i injection valve (5 mL loading loop), a Waters 500 pump, and a Waters 490E programmable wavelength detector operating at 214 and 230 nm.

Purity was determined by analysis of the ^{1}H NMR spectrum, reversed-phase HPLC and analysis of the total ion count on UPLC-MS. Exemplar analogues were selected for further saturation transfer difference NMR analysis to confirm the presence of rotamers.

Fmoc-SPPS General Protocols. Fmoc-SPPS procedures were employed on acid-labile 2-CTC within fritted syringes. All reagent equivalents are with respect to the amount of the initial amino acid loaded to resin.

Resin Loading. 2-CTC resin (1.33 mmol/g) was swelled in 5 vol % iPr$_2$NEt/CH_2Cl_2 (0.015 M) and shaken for 20 min. The solvent was discharged, and the resin was washed with CH_2Cl_2 (×5). The resin was treated with the desired Fmoc-amino acid or dipeptide (1−4 equiv in regard to the predicted resin loading) and iPr$_2$NEt (2−8 equiv) in CH_2Cl_2 (0.05 M) and shaken at room temperature for 16 h. The coupling solution was discharged and washed with CH_2Cl_2 (×5), DMF (×5), and CH_2Cl_2 (×5). The resin was treated with a capping solution of 17:2:1 (v/v/v) CH_2Cl_2/iPr$_2$NEt/MeOH and shaken at room temperature for 30 min. The capping solution was discharged, and the resin was washed with CH_2Cl_2 (×5) and DMF (×5).

Resin Loading Determination. The resin-bound peptide was treated with a solution of 10 vol % piperidine/DMF (2 × 3 min). The deprotection solution was discharged and collected, and the resin was washed with DMF (×5), CH_2Cl_2 (×5), and DMF (×5). The combined deprotection solutions were made up to 25 mL using 10 vol % piperidine/DMF and diluted 1:100 with 10 vol % piperidine/DMF. The amount of peptide loaded to resin was determined by the measurement of the UV absorbance at λ = 301 nm of the diluted deprotection solution.

Fmoc-Deprotection. The resin-bound peptide was treated with a solution of 10 vol % piperidine/DMF (2 × 3 min). The deprotection solution was discharged, and the resin was washed with DMF (×5), CH_2Cl_2 (×5), and DMF (×5).

HATU Coupling Conditions. The resin-bound peptide was treated with a solution of a given amino acid (4 equiv), HATU (4 equiv), and iPr$_2$NEt (8 equiv) in DMF (0.1 M in regard to the loaded peptide) and shaken for 2 h at room temperature. The coupling solution was discharged, and the resin was washed with DMF (×5), CH_2Cl_2 (×5), and DMF (×5).

HATU/HOAt Coupling Conditions (Coupling to *N*-Methylated Amino Acids). The resin-bound peptide was

https://doi.org/10.1021/acsinfecdis.5c00689
ACS Infect. Dis. XXXX, XXX, XXX−XXX

treated with a solution of a given amino acid (1.2−4 equiv), HATU (1.2−4 equiv), HOAt (2.4−8 equiv), and iPr$_2$NEt (2.4−8 equiv) in DMF (0.1 M in regards to the loaded peptide) and shaken for 8 h at room temperature. The coupling solution was discharged, and the resin was washed with DMF (×5), CH_2Cl_2 (×5), and DMF (×5).

On-Resin *N*-Methylation. The resin-bound peptide was treated with a solution of 2-nitrobenzenesulfonyl chloride (4 equiv) and 2,4,6-trimethylpyridine (10 equiv) in *N*-methyl-2-pyrrolidone (NMP) (0.1 M in regards to the loaded peptide) and shaken at room temperature for 20 min. The protection solution was discharged, and the resin was washed with DMF (×5), CH_2Cl_2 (×5), and THF (×10). The resin-bound peptide was treated with a solution of PPh_3 (5 equiv) and anhydrous MeOH (10 equiv) in anhydrous THF (0.2 M in regard to the loaded peptide). The resin was shaken at room temperature for 1 min at which point an additional solution of DIAD (5 equiv) in THF (0.2 M in regard to the loaded peptide) was sucked into the fritted syringe. The resin was shaken for 15 min, the solution was discharged, and the resin was washed with DMF (×5), CH_2Cl_2 (×5), and DMF (×5). The resin-bound peptide was treated with a solution of 1,8-diazabicyclo[5.4.0]undec-7-ene (5 equiv) and 2-mercaptoethanol (10 equiv) in NMP (0.1 M in regard to the loaded peptide) (2 × 5 min). The deprotection solution was discharged, and the resin was washed with DMF (×5), CH_2Cl_2 (×5), and DMF (×5).

On-Resin Alloc-Deprotection. The resin-bound peptide was washed with CH_2Cl_2 (×10) and treated with a solution of $Pd(PPh_3)_4$ (0.2 equiv) and phenylsilane (20 equiv) in CH_2Cl_2 (0.018 M in regards to the loaded peptide) and shaken at room temperature for 20 min. The deprotection solution was discharged, and the resin was washed with CH_2Cl_2 (×5) and DMF (×5).

Resin Cleavage Conditions. The resin-bound peptide was washed with CH_2Cl_2 (×10) and then treated with a solution of 30 vol % HFIP/CH_2Cl_2 (3 × 20 min). The cleavage solution was discharged, collected, and concentrated under a stream of N_2 and dried in vacuo.

Cyclization, Purification, and Deprotection Conditions A. PyBOP (5.3 equiv) was dissolved in CH_2Cl_2 (0.0008 M), and to this solution was added iPr$_2$NEt (5.3 equiv). The protected linear peptide (1 equiv) was dissolved in CH_2Cl_2 (0.0013 M) and added dropwise to the solution of PyBOP and iPr$_2$NEt over 16 h at room temperature while stirring. The cyclization solution was concentrated in vacuo. The crude cyclic peptide was redissolved in iPr$_3$SiH/TFA/CH_2Cl_2 (2:49:49, v/v/v, 5 mL) and stirred at room temperature for 1 h. The deprotection solution was concentrated under a stream of N_2 and redissolved in MeCN/H_2O (1:1, v/v, 5 mL), and to this solution was added two drops of AcOH. The solution was stirred at room temperature for 16 h and subsequently purified by reversed-phase HPLC.

Cyclization, Purification, and Deprotection Conditions B. PyBOP (5.3 equiv) was dissolved in CH_2Cl_2 (0.0008 M), and to this solution was added iPr$_2$NEt (5.3 equiv). The protected linear peptide (1 equiv) was dissolved in CH_2Cl_2 (0.0013 M) and added dropwise to the solution of PyBOP and iPr$_2$NEt over 16 h at room temperature while stirring. The cyclization solution was concentrated in vacuo. The crude cyclic peptide was purified by normal-phase flash chromatography (0−50% v/v acetone in *n*-hexane or pentane) to afford the purified cyclic peptide. This peptide was dissolved in iPr$_3$SiH/TFA/CH_2Cl_2 (2:49:49, v/v/v, 5 mL) and stirred at room temperature for 1 h. The deprotection solution was concentrated under a stream of N_2 and redissolved in MeCN/H_2O (1:1, v/v, 5 mL), and to this solution was added two drops of AcOH. The solution was stirred at room temperature for 16 h and then lyophilized three times to afford the deprotected cyclic peptide.

Cyclization, Purification, and Deprotection Conditions C. PyBOP (5.3 equiv) was dissolved in CH_2Cl_2 (0.0008 M) and to this solution was added iPr$_2$NEt (5.3 equiv). The protected linear peptide (1 equiv) was dissolved in CH_2Cl_2 (0.0013 M) and added dropwise to the solution of PyBOP and iPr$_2$NEt over 16 h at 40 °C while stirring. The cyclization solution was concentrated in vacuo. The crude cyclic peptide was purified by normal-phase flash chromatography (0−50% v/v acetone in *n*-hexane or pentane) to afford the purified cyclic peptide. This peptide was dissolved in 4 M HCl/1,4-dioxane (1 mL) and stirred at room temperature for 16 h. The deprotection solution was lyophilized to afford the purified and deprotected cyclic peptide.

Solution-phase Carboxylic acid Coupling. PyBOP (4 equiv), the desired carboxylic acid (2 equiv) and *N*-methylmorpholine (5 equiv) were added to a solution of the desired peptide in DMF (0.008 M). The resulting solution was then stirred at room temperature for 2 h and then diluted with water for injection onto the RP-HPLC.

SPPS Reaction Monitoring. Following a coupling reaction, several beads were removed from the reaction vessel and treated with a solution of 10 vol % piperidine/DMF (2 × 3 min). The deprotection solution was discharged, and the beads were washed with DMF (×5), CH_2Cl_2 (×5), and DMF (×5). The beads were then treated with a solution of 95:2.5:2.5 (v/v/v) TFA/iPr$_3$SiH/H_2O (1 mL) and shaken for 20 min at room temperature or 30 vol % HFIP in CH_2Cl_2 and shaken for 2 min at room temperature. The solution was discharged and concentrated under nitrogen and redissolved in 1:1 (v/v) MeCN/H_2O and injected into the UPLC−MS system. Conversion of starting material into the product was then monitored, and couplings were determined to be complete following the disappearance of starting material.

Detailed experimental and characterization for all amino acids, peptides and natural product analogues can be found in the Supporting Information file.

Expression and Purification of Mtb ClpC1. *Mtb* ClpC1-NTD$_{1-148}$ was expressed in *Escherichia coli* (*E. coli*) cells. A DNA gBlock for C-terminal His$_6$-tagged ClpC1-NTD was cloned into pET28a plasmids then transformed into *E. coli* DH5α competent cells. Plasmids containing His$_6$-tagged proteins were transformed into *E. coli* BL21(DE3) for large scale expression in LB media supplemented with kanamycin. Cultures were incubated at 37 °C until OD_{600} ∼ 0.8 and expression was induced with 0.5 mM isopropyl β-thiogalactopyranoside (IPTG). Expression cultures were transferred to 18 °C and incubated for a further ∼20 h. Cells were harvested by centrifugation at 5000 g at 4 °C for 30 min. Pellets were resuspended with lysis buffer (10 mM Tris pH 7.5, 150 mM NaCl, 1× cOmplete protease inhibitor EDTA-free [Roche] and lysozyme) and lysed with sonication.

Recombinant protein was purified from lysate by nickel-nitrilotriacetic acid (Ni-NTA) affinity chromatography and fractions were analyzed by sodium dodecyl sulfate-polyacrylamide gel electrophoresis (SDS−PAGE). Discrete fractions of the correct molecular weight were pooled, concentrated, and

https://doi.org/10.1021/acsinfecdis.5c00689
ACS Infect. Dis. XXXX, XXX, XXX−XXX

loaded onto a size exclusion chromatography (SEC) column (Hiload, Superdex200 10/300, GE healthcare) equilibrated with SEC buffer containing 150 mM NaCl, 50 mM NaPi, pH 8. Purification was monitored by SDS−PAGE. Discrete fractions were pooled, concentrated, flash frozen with liquid nitrogen, and stored at −80 °C.

Surface Plasmon Resonance. SPR was used to measure the binding affinities of peptides **4**−**9** and **19**−**38** to recombinant *Mtb* ClpC1-NTD$_{1-148}$. SPR measurements were carried out using a Biacore T200 (GE Healthcare), and data analysis undertaken using the Biacore Insight Evaluation Software. Experiments were performed in single cycle kinetics mode at 25 °C. The sensor chip surface of a CM5 chip (Cytiva) was activated using a 1:1 mix of 1-ethyl-3-(3-(dimethylamino)propyl) carbodiimide hydrochloride and *N*-hydroxysuccinimide. ClpC1-NTD (200 nM) in sodium acetate buffer (10 mM, pH 4.0) was immobilized to a target density of 1600 RU. Ethanolamine (1 M) was used to quench any remaining *N*-hydroxysuccinimide esters on the surface of flow cells. A solution composed of 25 mM Tris, 150 mM NaCl, 0.1% DMSO (v/v), 0.01% Tween-20 (v/v) at pH 7.5 was used as the running buffer. Peptides were injected as a concentration series (123, 370, 1110, 3330, and 10000 nM) with a contact time of 120 s and a dissociation time of 1200 s at a flow rate of 50 μL/min. Data were then reference subtracted and blank subtracted prior to processing. Equilibrium dissociation constants (K_D) were calculated assuming 2:1 binding, as exploited in the Biacore T200 Evaluation software (kinetic heterogeneous ligand model). This model provided two calculated binding constants (K_{D1} and K_{D2}); only the highest affinity binding constant measured has been tabulated (see ESI for sensorgrams and K_{D1} and K_{D2} values). Data are expressed as the mean of measurements performed in triplicate (sensorgrams with calculated dissociation constants expressed as mean ± SEM are provided in the Supporting Information).

MIC Determination and Kinetics of Cell Killing. The avirulent auxotrophic *Mtb* strain mc^{2}6230 (Δ*RD1* Δ*panCD*) was used to monitor the kinetics of cell killing by the analogues. Isoniazid and ecumicin (**2**) were used as a positive control. Strain mc^{2}6230 (Δ*RD1* Δ*panCD*) is an avirulent auxotrophic *Mtb* mutant that behaves identically to wild-type *Mtb* when grown in pantothenate-supplemented medium but is incapable of causing disease even in SCID mice.[34] Growth of *Mtb* strain mc^{2}6230 was grown in Middlebrook 7H9 broth supplemented with OADC (0.005% oleic acid, 0.5% bovine serum albumin, 0.2% dextrose, and 0.085% catalase), 0.05% tyloxapol (Sigma), and 25 μg/mL pantothenic acid (PAN). Cultures were maintained in 10 mL volumes in 30 mL inkwells at 37 °C with agitation (140 rpm). When required, mc^{2}6230 was grown on Middlebrook 7H11 agar supplemented with OADC and PAN.

The MIC values for the analogues, ecumicin (**2**), and isoniazid were determined by inoculating *Mtb* into 96-well plates containing supplemented Middlebrook 7H9 broth, at a starting OD$_{600}$ of 0.05, in a total starting volume of 100 μL. Test compounds were dispensed from a 9-point, 2-fold dilution gradient to each well, with a maximum of 2% dimethyl sulfoxide (DMSO). MIC assay 96-well plates were incubated without shaking at 37 °C for 10 days. On day 7, OD$_{600}$ values were measured in a Varioskan LUX (Thermo Fisher Scientific) microplate reader, and MIC values were determined in biological triplicates.

To determine the effects of test compounds on the cell killing of *Mtb*, cells were grown in 10 mL volumes in 30 mL inkwells at 37 °C with agitation (140 rpm). When cells reached an OD$_{600}$ of 0.5 (time zero, approximately 1 × 10^8 CFU/mL), the cultures were challenged with 10× the MIC of the test compound and cell viability monitored for 28 days by sampling at various time points (as indicated). Cultures were taken and diluted along a seven-point 10-fold dilution curve with 5 μL spotted onto 7H11 agar, and colony-forming units (CFU/mL) determined after 4 weeks of incubation at 37 °C. All experiments were performed in biological triplicates, and the standard error of the mean is shown.

Measurement of ClpC1-Mediated Casein Degradation by the ClpP1P2 Protease Complex. To test the effect of ecumicin and analogues on substrate degradation by the mycobacterial ClpC1P1P2, in vitro degradation assays were carried out. Hexameric *M. smegmatis* ClpC1 (0.5 μM) together with mature (14-mer complex after pro-peptide cleavage) *M. smegmatis* ClpP1P2 (0.3 μM) was incubated shortly with either 100 μM (dissolved in DMSO) of ecumicin, analogues or cyclomarin A (diluted from 10 mM DMSO stocks) in comparison to a DMSO control. A final DMSO concentration of 1% was used for all conditions. The assay was set up using 15 μM ß-casein, 20 mM phosphoenolpyruvate (PEP) and 10 U/ml pyruvate kinase (Sigma-Aldrich) in a buffer containing 50 mM HEPES pH 7.5, 100 mM KCl, 10 mM $MgCl_2$ and 10% glycerol. To start the reaction, ATP was added to a final concentration of 5 mM and the reaction was incubated at 37 °C. Time points of 5 μL were taken before reaction start and then each after 30 and 60 min. To stop the reaction, SDS sample buffer was added prior to an SDS−PAGE and Coomassie staining.

Measurement of ClpC1 ATPase Activity. To test the in vitro ATPase activity of ClpC1, an ATP/NADH assay was applied to monitor decreasing levels of NADH in the reaction, driven by lactate dehydrogenase (LDH) mediated processing of pyruvate. Addition of an ATP regeneration system with pyruvate kinase (PK) and phosphoenolpyruvate (PEP) provides a readout that directly correlates NADH decrease with ATP consumption. Hexameric *M. smegmatis* ClpC1 (0.75 μM) was preincubated for 20 min with 100 μM (dissolved in DMSO) of either analogues or cyclomarin A (diluted from 10 mM DMSO stocks) in comparison to a DMSO control. A final DMSO concentration of 1% was used for all conditions. A working solution including PEP (1 mM), LDH (15 U/ml), PK (15 U/ml), $MgCl_2$ (20 mM), NADH (0.4 mM) and ATP (10 mM) was added to each reaction, in a buffer containing 50 mM HEPES pH 7.5, 100 mM KCl, 10 mM $MgCl_2$ and 10% glycerol. NADH levels were monitored spectrophotometrically (PHERAstar FSX) for 30 min after addition of the working solution. NADH concentration was calculated by additionally measuring a NADH calibration curve (0.06, 0.13, 0.25, and 0.5 mM), which was used to determine ΔA/μM NADH. From ClpC1 measurements, the linear region of the curve was fitted to obtain ΔA/min, which was converted to μM NADH/min. Division by six yielded the ATP consumption rate per ClpC1 hexamer.

In Vivo Study. Zebrafish embryos were produced by natural spawning in accordance with Sydney Local Health District Animal Welfare Committee Approval 17-036. Two days post fertilization embryos were infected with approximately 200 fluorescent *M. marinum* M strain by microinjection into the caudal vein as per Matty et al.[37] Embryos

https://doi.org/10.1021/acsinfecdis.5c00689
ACS Infect. Dis. XXXX, XXX, XXX−XXX

were maintained in E3 media supplemented with 45 μg/mL 1-phenyl-2-thiourea to prevent pigmentation and treated with compounds by immersion, as indicated. Images of infected embryos were captured using a Leica M205FA fluorescent microscope, and burden was measured using fluorescent pixel count.[37]

■ ASSOCIATED CONTENT

Supporting Information

The Supporting Information is available free of charge at https://pubs.acs.org/doi/10.1021/acsinfecdis.5c00689.

Gelelectrophoresis of exemplar analogues, ecumicin, cyclomarin A, and DMSO controls in the degradation assay of β-casein; analytical HPLC traces and the corresponding MS of cyclic peptide analogues; SPR sensorgrams; synthesis of Fmoc-L-DABA(Alloc)−OH (**11**), 5-(*tert*-butoxycarbonyl)amino)pentanoic acid (**S8**), and 5-((*tert*-butoxycarbonyl)(methyl)amino)-pentanoic acid (**S9**); NMR assignments and selective chemical exchange for analogues **5**, **8**, **25**, and **37**; and 1D- and 2D-NMR spectra (PDF)

■ AUTHOR INFORMATION

Corresponding Author

Richard J. Payne − *School of Chemistry and Australian Research Council Centre of Excellence for Innovations in Peptide and Protein Science, The University of Sydney, Sydney, NSW 2006, Australia;* orcid.org/0000-0002-3618-9226; Email: richard.payne@sydney.edu.au

Authors

Paige M. E. Hawkins − *School of Chemistry and Australian Research Council Centre of Excellence for Innovations in Peptide and Protein Science, The University of Sydney, Sydney, NSW 2006, Australia;* orcid.org/0000-0002-5829-1977

Max J. Bedding − *School of Chemistry and Australian Research Council Centre of Excellence for Innovations in Peptide and Protein Science, The University of Sydney, Sydney, NSW 2006, Australia*

David M. Hoi − *Research Institute of Molecular Pathology (IMP), 1030 Vienna, Austria*

Isabel K. Barter − *School of Chemistry and Australian Research Council Centre of Excellence for Innovations in Peptide and Protein Science, The University of Sydney, Sydney, NSW 2006, Australia*

Chen-Yi Cheung − *Department of Microbiology and Immunology, School of Biomedical Sciences, University of Otago, Dunedin 9054, New Zealand*

Stefan H. Oehlers − *Tuberculosis Research Program at the Centenary Institute, The University of Sydney, Camperdown, NSW 2050, Australia; A*STAR Infectious Diseases Laboratories (A*STAR ID Laboratories), Agency for Science, Technology and Research (A*STAR), Singapore 138648, Singapore*

Gregory M. Cook − *Department of Microbiology and Immunology, School of Biomedical Sciences, University of Otago, Dunedin 9054, New Zealand;* orcid.org/0000-0001-8349-1500

Tim Clausen − *Research Institute of Molecular Pathology (IMP), 1030 Vienna, Austria*

Warwick J. Britton − *Tuberculosis Research Program at the Centenary Institute, The University of Sydney, Camperdown, NSW 2050, Australia; Department of Clinical Immunology, Royal Prince Alfred Hospital, Camperdown, NSW 2050, Australia*

Complete contact information is available at: https://pubs.acs.org/10.1021/acsinfecdis.5c00689

Notes

The authors declare no competing financial interest.

■ ACKNOWLEDGMENTS

We would like to acknowledge funding from the National Health and Medical Research Council (Ideas Grant APP2038610 and Tuberculosis Centre of Research Excellence APP1153493 to W.J.B.). The authors also acknowledge the Research Training Program and the John A. Lamberton Research Scholarship for PhD funding (to P. H.). GMC and CYC are funded by the Health Research Council of New Zealand. We would like to thank Dr. Julia Leodolter (Research Institute of Molecular Pathology, Vienna, Austria) for useful discussions around Clp complex formation and assays. We would also like to thank Dr. Ian Luck (Sydney Analytical, The University of Sydney) for technical support with NMR spectroscopy, Dr. Nick Proschogo (The University of Sydney) for technical support with mass spectrometry and the microscopy facilities of the BioImaging Facility and Sydney Cytometry at Centenary Institute.

■ ABBREVIATIONS

Ac, acetyl; Alloc, allyloxycarbonyl; ATP, adenosine triphosphate; Bn, benzyl; Boc, *tert*-butoxycarbonyl; CFU, colony-forming unit; ClpC1, caseinolytic protease C1; 2-CTC, 2-chlorotrityl; DABA, (2*S*,3*R*) 2,3 diaminobutanoic acid; DAP, 2,3-diaminopropionic acid; DBU, 1,8-diazabicyclo[5.4.0]-undec-7-ene; DIAD, di*iso*propyl azodicarboxylate; DMF, dimethylformamide; DMSO, dimethyl sulfoxide; EDC, 1-ethyl-3-(3-(dimethylamino)propyl)carbodiimide; ESI, electrospray ionization; Fmoc, 9-fluorenylmethoxycarbonyl; HATU, 1-[*bis*(dimethylamino)methylene]-1*H*−1,2,3-triazolo[4,5b]-pyridinium 3-oxid hexafluorophosphate; HFIP, 1,1,1,3,3,3-hexafluoroisopropanol; HOAt, 1-hydroxyazabenzotriazole; HOBt, 1-hydroxybenzotriazole; RP-HPLC, reversed-phase-high-performance liquid chromatography; HR-MS, high-resolution mass spectrometry; HMBC, heteronuclear multiple bond correlation; HSQC, heteronuclear single quantum coherence; IR, Infrared; LR-MS, low-resolution mass spectrometry; MDR, multidrug-resistant; MIC, minimum inhibitory concentration; *Msm*, *Mycobacterium smegmatis*; *Mtb*, *Mycobacterium tuberculosis*; NMM, *N*-methylmorpholine; NMP, *N*-methyl-2-pyrrolidone; NMR, nuclear magnetic resonance; Ns, 4-nitrobenzenesulfonyl; NTD, N-terminal domain; Nv, 4,5-dimethoxy-2-nitrobenzyl; OD_{600}, optical density at 600 nm; PyBOP, benzotriazol-1-yloxytripyrrolidino-phosphonium hexafluorophosphate; SAR, structure−activity relationship; SCID, severe combined immunodeficiency; SPPS, solid-phase peptide synthesis; SPR, surface plasmon resonance; STD, saturation transfer difference; TB, tuberculosis; TFA, trifluoroacetic acid; THF, tetrahydrofuran; TLC, thin-layer chromatography; TsOH, *p*-toluenesulfonic acid; UPLC-MS, ultraperformance liquid chromatography−mass spectrometry; XDR, extensively drug-resistant

https://doi.org/10.1021/acsinfecdis.5c00689
ACS Infect. Dis. XXXX, XXX, XXX−XXX

REFERENCES

(1) World Health Organization, "Global tuberculosis report 2024" can be found at https://www.who.int/global-programme-on-tuberculosis-and-lung-health/tb-reports/global-tuberculosis-report-2024, 2024.

(2) United Nations, Political Declaration Of The UN General Assembly High-Level Meeting can be found at https://www.who.int/tb/unhlmonTBDeclaration.pdf, 2018.

(3) United Nations, Transforming our World: The 2030 Agenda for Sustainable Development can be found at https://sdgs.un.org/publications/transforming-our-world-2030-agenda-sustainable-development-17981, 2015.

(4) World Health Organization, The End TB Strategy can be found at https://www.who.int/publications/i/item/WHO-HTM-TB-2015.19, 2015.

(5) United Nations, Progress towards the achievement of global tuberculosis targets and implementation of the political declaration of the high-level meeting of the General Assembly on the fight against tuberculosis can be found at https://undocs.org/en/A/75/236, 2020.

(6) World Health Organization, WHO consolidated guidelines on tuberculosis, Module 4: treatment and care can be found at https://www.who.int/publications/i/item/9789240107243, 2025.

(7) Blair, J. M.; Webber, M. A.; Baylay, A. J.; Ogbolu, D. O.; Piddock, L. J. Molecular Mechanisms of Antibiotic Resistance. *Nat. Rev. Microbiol.* **2015**, *13* (1), 42−51.

(8) Brown, E. D.; Wright, G. D. Antibacterial Drug Discovery in the Resistance Era. *Nature* **2016**, *529* (7586), 336−343.

(9) Um, S.; Choi, T. J.; Kim, H.; Kim, B. Y.; Kim, S. H.; Lee, S. K.; Oh, K. B.; Shin, J.; Oh, D.-C. Ohmyungsamycins A and B: Cytotoxic and Antimicrobial Cyclic Peptides Produced by *Streptomyces* sp. from a Volcanic Island. *J. Org. Chem.* **2013**, *78*, 12321−12329.

(10) Kim, T. S.; Shin, Y. H.; Lee, H. M.; Kim, J. K.; Choe, J. H.; Jang, J. C.; Um, S.; Jin, H. S.; Komatsu, M.; Cha, G. H.; Chae, H. J.; Oh, D. C.; Jo, E. K. Ohmyungsamycins Promote Antimicrobial Responses Through Autophagy Activation via AMP-Activated Protein Kinase Pathway. *Sci. Rep.* **2017**, *7* (1), 3431.

(11) Hawkins, P. M. E.; Tran, W.; Nagalingam, G.; Cheung, C. Y.; Giltrap, A. M.; Cook, G. M.; Britton, W. J.; Payne, R. J. Total Synthesis and Antimycobacterial Activity of Ohmyungsamycin A, Deoxyecumicin, and Ecumicin. *Chem.—Eur. J.* **2020**, *26* (66), 15200−15205.

(12) Hur, J.; Jang, J.; Sim, J.; Son, W. S.; Ahn, H. C.; Kim, T. S.; Shin, Y. H.; Lim, C.; Lee, S.; An, H.; Kim, S. H.; Oh, D. C.; Jo, E. K.; Jang, J.; Lee, J.; Suh, Y. G. Conformation-Enabled Total Syntheses of Ohmyungsamycins A and B and Structural Revision of Ohmyungsamycin B. *Angew. Chem., Int. Ed. Engl.* **2018**, *57* (12), 3069−3073.

(13) Gao, W.; Kim, J. Y.; Chen, S. N.; Cho, S. H.; Choi, J.; Jaki, B. U.; Jin, Y. Y.; Lankin, D. C.; Lee, J. E.; Lee, S. Y.; McAlpine, J. B.; Napolitano, J. G.; Franzblau, S. G.; Suh, J. W.; Pauli, G. F. Discovery and Characterization of the Tuberculosis Drug Lead Ecumicin. *Org. Lett.* **2014**, *16* (23), 6044−6047.

(14) Gao, W.; Kim, J. Y.; Anderson, J. R.; Akopian, T.; Hong, S.; Jin, Y. Y.; Kandror, O.; Kim, J. W.; Lee, I. A.; Lee, S. Y.; McAlpine, J. B.; Mulugeta, S.; Sunoqrot, S.; Wang, Y.; Yang, S. H.; Yoon, T. M.; Goldberg, A. L.; Pauli, G. F.; Suh, J. W.; Franzblau, S. G.; Cho, S. The Cyclic Peptide Ecumicin Targeting ClpC1 is Active Against *Mycobacterium tuberculosis* In Vivo. *Antimicrob. Agents Chemother.* **2015**, *59* (2), 880−889.

(15) Hawkins, P. M. E.; Giltrap, A. M.; Nagalingam, G.; Britton, W. J.; Payne, R. J. Total Synthesis of Ecumicin. *Org. Lett.* **2018**, *20* (4), 1019−1022.

(16) Gao, W.; McAlpine, J. B.; Choules, M. P.; Napolitano, J. G.; Lankin, D. C.; Simmler, C.; Ho, N. A.; Lee, H.; Suh, J. W.; Burton, I. W.; Cho, S.; Franzblau, S. G.; Chen, S. N.; Pauli, G. F. Structural Sequencing of Oligopeptides Aided by ^{1}H Iterative Full-Spin Analysis. *J. Nat. Prod.* **2017**, *80* (10), 2630−2643.

(17) Wolf, N. M.; Lee, H.; Zagal, D.; Nam, J. W.; Oh, D. C.; Lee, H.; Suh, J. W.; Pauli, G. F.; Cho, S.; Abad-Zapatero, C. Structure of the N-Terminal Domain of ClpC1 in Complex with the Antituberculosis Natural Product Ecumicin Reveals Unique Binding Interactions. *Acta Cryst. D. Struct. Biol.* **2020**, *76* (5), 458−471.

(18) Lupoli, T. J.; Vaubourgeix, J.; Burns-Huang, K.; Gold, B. Targeting the Proteostasis Network for Mycobacterial Drug Discovery. *ACS Infect. Dis.* **2018**, *4* (4), 478−498.

(19) Bhandari, V.; Wong, K. S.; Zhou, J. L.; Mabanglo, M. F.; Batey, R. A.; Houry, W. A. The Role of ClpP Protease in Bacterial Pathogenesis and Human Diseases. *ACS Chem. Biol.* **2018**, *13* (6), 1413−1425.

(20) Culp, E.; Wright, G. D. Bacterial Proteases, Untapped Antimicrobial Drug Targets. *J. Antibiot.* **2017**, *70* (4), 366−377.

(21) Krüger, E.; Witt, E.; Ohlmeier, S.; Hanschke, R.; Hecker, M. The Clp Proteases of *Bacillus subtilis* are Directly Involved in Degradation of Misfolded Proteins. *J. Bacteriol.* **2000**, *182* (11), 3259−3265.

(22) Stahlhut, S. G.; Alqarzaee, A. A.; Jensen, C.; Fisker, N. S.; Pereira, A. R.; Pinho, M. G.; Thomas, V. C.; Frees, D. The ClpXP Protease is Dispensable for Degradation of Unfolded Proteins in *Staphylococcus aureus*. *Sci. Rep.* **2017**, *7*, 11739.

(23) Hong, J.; Duc, N. M.; Jeong, B.-C.; Cho, S.; Shetye, G.; Cao, J.; Lee, H.; Jeong, C.; Lee, H.; Suh, J.-W. Identification of the Inhibitory Mechanism of Ecumicin and Rufomycin 4−7 on the Proteolytic Activity of *Mycobacterium tuberculosis* ClpC1/ClpP1/ClpP2 Complex. *Tuberculosis* **2023**, *138*, No. 102298.

(24) Hoi, D. M.; Junker, S.; Junk, L.; Fischel, K.; Podlesainski, D.; Schwechel, K.; Kasani, F.; van Geelen, L.; Leodolter, J.; Hawkins, P.; Morreale, F. E.; Kleine, S.; Guha, S.; Rumpel, K.; Schmiedel, V. M.; Weinstabl, H.; Meinhart, A.; Kalscheuer, R.; Payne, R. J.; Kaiser, M.; Hartl, M.; Boehmelt, G.; Kazmaier, U.; Clausen, T. Clp-Targeting BacPROTACs Impair Mycobacterial Proteostasis and Survival. *Cell* **2023**, *186* (10), 2176.

(25) Hawkins, P. M. E.; Hoi, D. M.; Cheung, C.-Y.; Wang, T.; Quan, D.; Sasi, V. M.; Liu, D. Y.; Linington, R. G.; Jackson, C. J.; Oehlers, S. H.; Cook, G. M.; Britton, W. J.; Clausen, T.; Payne, R. J. Potent Bactericidal Antimycobacterials Targeting the Chaperone ClpC1 Based on the Depsipeptide Natural Products Ecumicin and Ohmyungsamycin A. *J. Med. Chem.* **2022**, *65* (6), 4893−4908.

(26) Stevens, M. T.; Hawkins, P. M. E.; Wang, T.; Payne, R. J.; Britton, W. J. Analogue of the Natural Product Ecumicin Causes Sustained Growth Inhibition of *Mycobacterium tuberculosis* Under Multiple Growth Conditions. *Tuberculosis* **2025**, *151*, No. 102594.

(27) Jolliffe, K. The Pseudoproline Approach to Peptide Cyclization. *Aust. J. Chem.* **2018**, *71*, 723.

(28) Tsuda, S.; Masuda, S.; Yoshiya, T. Epimerization-Free Preparation of C-Terminal Cys Peptide Acid by Fmoc SPPS Using Pseudoproline-Type Protecting Group. *J. Org. Chem.* **2020**, *85*, 1674.

(29) Wohr, T.; Wahl, F.; Nefzi, A.; Rohwedder, B.; Sato, T.; Sun, X. C.; Mutter, M. Pseudo-Prolines as a Solubilizing, Structure-Disrupting Protection Technique in Peptide Synthesis. *J. Am. Chem. Soc.* **1996**, *118*, 9218.

(30) Heinlein, C.; Varón Silva, D.; Tröster, A.; Schmidt, J.; Gross, A.; Unverzagt, C. Fragment Condensation of C-Terminal Pseudoproline Peptides without Racemization on the Solid Phase. *Angew. Chem., Int. Ed.* **2011**, *50*, 6406.

(31) Hosono, Y.; Uchida, S.; Shinkai, M.; Townsend, C. E.; Kelly, C. N.; Naylor, M. R.; Lee, H.-W.; Kanamitsu, K.; Ishii, M.; Ueki, R.; Ueda, T.; Takeuchi, K.; Sugita, M.; Akiyama, Y.; Lokey, S. R.; Morimoto, J.; Sando, S. Amide-to-Ester Substitution as a Stable Alternative to N-Methylation for Increasing Membrane Permeability in Cyclic Peptides. *Nat. Commun.* **2023**, *14*, 1416.

(32) Sélambarom, J.; Monge, S.; Carré, F.; Roque, J. P.; Pavia, A. A. Stereoelectronic Control of Oxazolidine Ring-Opening: Structural and Chemical Evidences. *Tetrahedron* **2002**, *58*, 9559.

(33) Biron, E.; Chatterjee, J.; Kessler, H. Optimized Selective N-Methylation of Peptides on Solid Support. *J. Pept. Sci.* **2006**, *12* (3), 213−219.

(34) Sambandamurthy, V. K.; Wang, X.; Chen, B.; Russell, R. G.; Derrick, S.; Collins, F. M.; Morris, S. L.; Jacobs, W. R., Jr A Pantothenate Auxotroph of *Mycobacterium tuberculosis* is Highly

https://doi.org/10.1021/acsinfecdis.5c00689
ACS Infect. Dis. XXXX, XXX, XXX−XXX

Attenuated and Protects Mice Against Tuberculosis. *Nat. Med.* **2002**, *8* (10), 1171−1174.
(35) Vilcheze, C.; Hartman, T.; Weinrick, B.; Jacobs, W. R., Jr. *Mycobacterium tuberculosis* is Extraordinarily Sensitive to Killing by a Vitamin C-Induced Fenton Reaction. *Nat. Commun.* **2013**, *4*, 1881.
(36) Cronan, M. R.; Tobin, D. M. Fit for Consumption: Zebrafish as a Model for Tuberculosis. *Dis. Model Mech.* **2014**, *7* (7), 777−784.
(37) Matty, M. A.; Oehlers, S. H.; Tobin, D. M. Live Imaging of Host-Pathogen Interactions in Zebrafish Larvae. *Methods Mol. Biol.* **2016**, *1451*, 207−223.

https://doi.org/10.1021/acsinfecdis.5c00689
ACS Infect. Dis. XXXX, XXX, XXX−XXX